High-resolution energy-filtered scanning tunneling microscopy using doped one-dimensional semiconductors

M. Mizuno and Eugene H. Kim
Department of Physics, University of Windsor, Windsor, Ontario, Canada N9B 3P4
(Received 21 October 2007; revised manuscript received 4 January 2008; published 13 February 2008)

We consider scanning tunneling microscopy (STM) using doped one-dimensional semiconducting tips. We show that these systems could be effective for high resolution energy-filtered STM, allowing one to probe the spectral function of surface states directly from the tunneling current. These systems would also allow for energy-resolved maps of surface states (with high energy resolution) using only constant-current imaging. A promising place to realize these effects is in doped semiconducting carbon nanotubes.

DOI: 10.1103/PhysRevB.77.085418 PACS number(s): 68.37.Ef, 73.20.At, 73.43.Jn, 73.63.−b

I. INTRODUCTION

Scanning tunneling microscopy (STM) has become a key technique for materials characterization; it has found utility in a variety of disciplines such as physics, chemistry, material science, and even biology.[1,2] More recently, STM has become instrumental for imaging and obtaining spectroscopic information at the atomic scale.[3] This technique has found utility in such diverse areas because it allows one to obtain three-dimensional, real space images; unlike other techniques, STM allows for good spatial resolution under conditions which do not destroy the sample being studied.[1]

In STM, electrons are made to tunnel from a "probe tip" into a sample under investigation; the tunneling current gives information about the surface of the sample. Since its invention,[4] a sharpened metal wire has typically been used as the probe tip. The use of a metal tip, however, limits the control one has over the states which contribute to the tunneling current.[1] Recently, it has been suggested that semiconducting (SC) probe tips could be very effective in STM—they would allow for *energy-filtered imaging*, where the tunneling current is determined only by states within a narrow energy interval.[5] This offers the exciting possibility of energy-resolved maps of sample states in constant-current mode (as compared to a metal tip which requires derivative spectroscopy for energy-resolved information[1,2,6]).

In this work, we consider doped one-dimensional (1D) semiconductors as STM tips. In one dimension, there is a singularity in the density of states (DOS) at the top and/or bottom of the valence and/or conduction band. In Ref. 7, it was shown that this singularity in the DOS could substantially influence the tunneling current. Here, we show that the interplay of band edge physics and the singularity in the DOS can be effective for energy-filtered STM and, in particular, could allow for high energy resolution. A promising place to realize these effects is in doped SC carbon nanotubes.[8] Indeed, recent work has demonstrated the utility of carbon nanotubes as STM tips—atomic resolution of a Si(111)-7×7 surface was achieved, with a measured tunneling current of approximately 0.5 nA.[9]

The rest of this paper is organized as follows. In Sec. II, we describe the STM setup and the systems considered. In Sec. III, we present our results for the tunneling current; we discuss the energy filtered STM from 1D and three-dimensional (3D) SC tips. In Sec. IV, we present a discussion of our results and some concluding remarks. Calculations of the spectral functions for the systems considered are outlined in the Appendix.

II. SYSTEM AND TUNNELING CURRENT

The energetics of our setup is shown in Fig. 1(a)—a scanning tunneling microscope with a doped SC tip is in contact with a sample which one is interested in probing. The semiconductor has an energy gap 2Δ between the valence and conduction bands; the valence band is filled with holes to an energy η. A voltage V is applied to the STM tip, shifting its spectrum relative to the sample. As discussed above, we will be interested in the case where the STM tip is a 1D semiconductor. Assuming the dopant atoms to be uniformly distributed (such that its band structure is not affected), we take the DOS of the 1D semiconductor to be

$$\mathcal{D}(\varepsilon) = \frac{\mathcal{D}_1}{2\pi} \mathrm{Re}\left[\frac{|\varepsilon - \Delta - \eta|}{\sqrt{(\varepsilon - \Delta - \eta)^2 - \Delta^2}}\right]. \quad (1)$$

The effects of the dopant atoms (impurities) are incorporated into a self-energy in the electron's spectral function—we assume a spectral function of the form

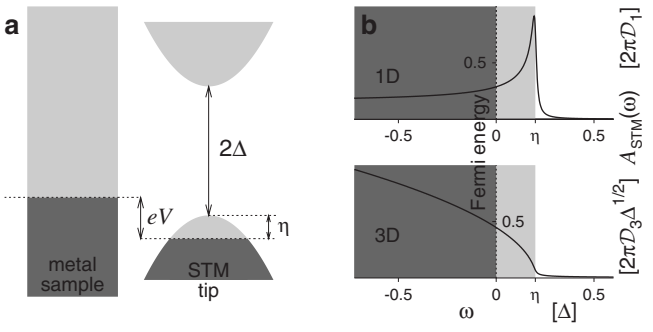

FIG. 1. (a) Setup: a scanning tunneling microscope with a doped SC tip (shown as parabolas) is in contact with a metal sample. The semiconductor has an energy gap 2Δ; the valence band is filled with holes to an energy η. (The dark shaded regions represent energy states filled with electrons.) A voltage V is applied to the STM tip, shifting its spectrum relative to the metal sample. (b) Top and bottom panel: shown in a solid line is the spectral function of 1D and 3D semiconductors. The dark shaded regions represent the energies of the valence band filled with electrons.

$$A(\epsilon,\omega) = \frac{2\Gamma}{(\omega-\epsilon)^2+\Gamma^2}, \tag{2}$$

where Γ is the scattering rate due to the impurities; for simplicity, we take Γ to be constant. Physically, larger values of Γ describe more disordered materials. In what follows, we take $\Gamma=0.01\Delta$. For comparison, we will also consider the case where the STM tip is a hole-doped 3D semiconductor. Here, we take the DOS to be

$$\mathcal{D}(\varepsilon) = \mathcal{D}_3 \,\mathrm{Re}[\sqrt{\eta-\varepsilon}], \tag{3}$$

we assume the electrons' spectral function to be given by Eq. (2). To simplify things a bit, we ignore the electrons' spin. This does not change our conclusions (which are determined by the electrons' DOS), but it simplifies some of the formulas.

An object which plays an important role is the STM's (local) spectral function $A_{\mathrm{STM}}(\omega)$, which is obtained by convolving the DOS with the electrons' spectral function,

$$A_{\mathrm{STM}}(\omega) = \int d\epsilon \mathcal{D}(\epsilon) A(\epsilon,\omega). \tag{4}$$

Performing the integral in Eq. (4) with $\mathcal{D}(\epsilon)$ given by Eq. (1) and $A(\epsilon,\omega)$ in Eq. (2), we obtain

$$A_{\mathrm{STM}}(\omega) = \frac{\mathcal{D}_1}{\sqrt{2}} \frac{|\Omega|\sqrt{1+\cos\theta}+\Gamma\sqrt{1-\cos\theta}}{[(\Omega^2-\Delta^2-\Gamma^2)^2+4\Gamma^2\Omega^2]^{1/4}}, \tag{5}$$

where

$$\cos\theta = \frac{(\Omega^2-\Delta^2-\Gamma^2)}{\sqrt{(\Omega^2-\Delta^2-\Gamma^2)^2+4\Gamma^2\Omega^2}},$$

with $\Omega=\omega-\Delta-\eta$. For the 3D SC tip, we perform the integral in Eq. (4) with $\mathcal{D}(\epsilon)$ given by Eq. (3) and $A(\epsilon,\omega)$ in Eq. (2), we obtain

$$A_{\mathrm{STM}}(\omega) = \pi\sqrt{2}\mathcal{D}_3[\sqrt{(\eta-\omega)^2+\Gamma^2}+\eta-\omega]^{1/2}. \tag{6}$$

$A_{\mathrm{STM}}(\omega)$ for the 1D and 3D SC tips are shown in Fig. 1(b). Notice that $A_{\mathrm{STM}}(\omega)$ for the 1D semiconductor has a singularity at the top of the valence band; $A_{\mathrm{STM}}(\omega)$ for the 3D semiconductor, on the other hand, goes to zero at the top of the valence band. As will be discussed below, this difference plays an important role in the energy resolution that can be achieved.

To discuss the physics of energy-filtered STM and to illustrate the effectiveness of doped 1D semiconductors as STM tips, we consider the tunneling current for two systems. We first consider a "diatomic molecule" attached to a surface. To describe this system, we consider the Hamiltonian

$$H = \sum_{\mathbf{p}} \varepsilon_{\mathbf{p}} c_{\mathbf{p}}^\dagger c_{\mathbf{p}} + \sum_{i=1,2} \varepsilon_i d_i^\dagger d_i + V_0(d_1^\dagger d_2 + d_2^\dagger d_1) + \sum_{\mathbf{p},i=1,2} V_{\mathbf{p},i}(e^{-i\mathbf{p}\cdot\mathbf{r}_i} c_{\mathbf{p}}^\dagger d_i + d_i^\dagger c_{\mathbf{p}} e^{i\mathbf{p}\cdot\mathbf{r}_i}). \tag{7}$$

In Eq. (7), $c_{\mathbf{p}}$ destroys an electron of momentum $\mathbf{p}$ in the metal, d_i destroys an electron in atom i's orbital with energy ε_i (which is closest to the Fermi energy) and centered about $\mathbf{r}_i$, V_0 describes the hybridization between the orbitals on the two atoms, and $V_{\mathbf{p},i}$ is the coupling between the orbital on atom i and the state with momentum $\mathbf{p}$ in the metal. For simplicity, in what follows, we take $V_{\mathbf{p},1}=V_{\mathbf{p},2}=V_1/\sqrt{\mathrm{Vol}}$, where V_1=constant and Vol is the volume of the metal. With this form for the $\{V_{\mathbf{p},i}\}$, electronic resonances have a Breit-Wigner line shape.[6]

We also consider probing the vibrational spectra of an atom or molecule attached to a surface. This phenomena has attracted considerable attention, initiated by the work of Ref. 10. It is also relevant to the area of molecular electronics,[11] where the influence of vibrational modes have been observed in the current through molecular junctions.[12] To describe this system, we consider the Hamiltonian[13]

$$H = \sum_{\mathbf{p}} \varepsilon_{\mathbf{p}} c_{\mathbf{p}}^\dagger c_{\mathbf{p}} + \varepsilon_0 d^\dagger d + \frac{1}{2m}p^2 + \frac{m\Omega^2}{2}x^2 + \sum_{\mathbf{p}} V_{\mathbf{p}}(c_{\mathbf{p}}^\dagger d + d^\dagger c_{\mathbf{p}}) + g x d^\dagger d. \tag{8}$$

In Eq. (8), $c_{\mathbf{p}}$ destroys an electron of momentum $\mathbf{p}$ in the metal, d destroys an electron on the atom's and/or molecule's orbital with energy ε_0, which is closest to the Fermi energy, $V_{\mathbf{p}}$ is the coupling between the atom and/or molecule and the state with momentum $\mathbf{p}$ in the metal, x (p) is the position (momentum) operator of the vibrational mode, Ω is the frequency of the vibrational mode, and g is the coupling between the vibrational mode and the electrons on the atom and/or molecule. Similar to Eq. (7), we take, for simplicity, $V_{\mathbf{p}}=V_1/\sqrt{\mathrm{Vol}}$.

The tunneling current between the STM tip and an atom and/or molecule on the surface is[1,2]

$$I = e\int \frac{d\omega}{2\pi} A_{\mathrm{STM}}(\omega+eV) A_f(\omega) T(\omega,eV)[n_F(\omega+eV)-n_F(\omega)], \tag{9}$$

where $n_F(\omega)$ is the Fermi function and $A_{\mathrm{STM}}(\omega)$ and $A_f(\omega)$ are the spectral functions for the STM tip and the atom and/or molecule, respectively—$A_{\mathrm{STM}}(\omega)$ is given by Eq. (5) for the 1D SC tip and Eq. (6) for the 3D SC tip; $A_f(\omega) = -2\,\mathrm{Im}[G_f(\omega)]$, where

$$G_f(t) = -i\Theta(t)\langle\{f(t),f^\dagger(0)\}\rangle \tag{10}$$

is the atom's and/or molecule's retarded Green's function, with $\Theta(t)$ being the step function and $\{\cdot,\cdot\}$ denoting the anticommutator. [$G_f(\omega)$ for the diatomic molecule and for the vibrational modes of an atom and/or molecule are computed in the Appendix.] Furthermore, $T(\omega,eV)$ is the tunneling transmission probability for electrons of energy ω at an applied bias voltage V. In what follows, we will be interested in small bias voltages. Hence, following other works, we take $T(\omega,eV)$=const (within the energy regime we are considering).[1,2,6]

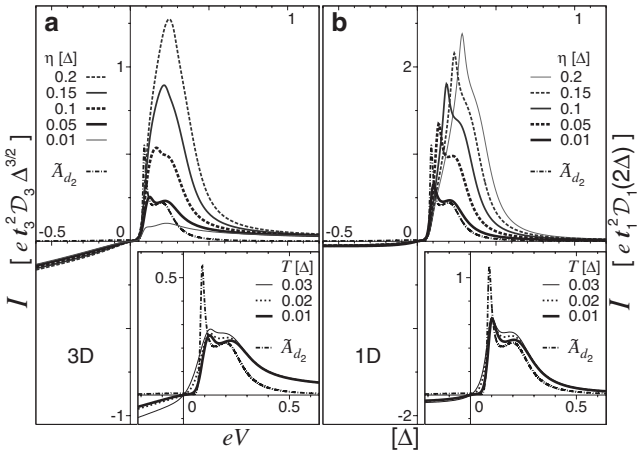

FIG. 2. *I-V* characteristics for the diatomic molecule. Parameters: $\varepsilon_1=-0.1\Delta$, $\varepsilon_2=-0.2\Delta$, $V_0=0.1\Delta$, $k_F r=0.05(2\pi)$, and $\gamma=0.05\Delta$. (a) Current (in units of $et^2\mathcal{D}_3\Delta^{3/2}$) vs bias voltage (in units of Δ) for a 3D SC tip for several values of η with $T=0.01\Delta$. (b) Current [in units of $et_1^2\mathcal{D}_1(2\Delta)$] vs bias voltage (in units of Δ) for a 1D SC tip for several values of η with $T=0.05\Delta$. Insets: current for several temperatures (with $\eta=0.01\Delta$). For comparison, $A_{d_2}(\omega)$ is shown in a dash-dotted line in units of the current and scaled by a factor—$A_{d_2}(\omega)$ is in units of $et_1^2\mathcal{D}_1 2\Delta/15\pi$ ($et_3^2\mathcal{D}_3\Delta^{3/2}/30\pi$) for the 1D (3D) SC tip.

III. RESULTS: HIGH RESOLUTION ENERGY-FILTERED STM

In this section, we discuss the tunneling current for the systems we are interested in probing Eqs. (7) and (8). Furthermore, we discuss in detail the energy filtered STM arising from 1D and 3D SC STM tips. In particular, we discuss the "mechanism" behind energy filtered STM; we discuss the factors which limit the resolution that can be achieved.

A. Tunneling current from a diatomic molecule

We begin by considering the diatomic molecule [Eq. (7)]. In what follows, we consider tunneling into the orbital on atom 2—$f=d_2$ in Eqs. (9) and (10); $G_{d_2}(\omega)$ is found to be

$$[G_{d_2}(\omega)]^{-1} = \omega - \varepsilon_2 + i\gamma - \frac{[V_0 - \gamma e^{ik_F r}/k_F r]^2}{\omega - \varepsilon_1 + i\gamma}. \quad (11)$$

with k_F being the Fermi wave vector, $r=|\mathbf{r}_2-\mathbf{r}_1|$, and $\gamma=\pi V_1^2\mathcal{D}_0$ ($\mathcal{D}_0$ is the DOS of the metal) [see the Appendix for details]. Figure 2 shows the tunneling current for the diatomic molecule—Figs. 2(a) and 2(b) are the current from a 3D and 1D SC tips. The values of the parameters were taken to be $\varepsilon_1=-0.1\Delta$, $\varepsilon_2=-0.2\Delta$, $V_0=0.1\Delta$, $k_F r=0.05(2\pi)$, and $\gamma=0.05\Delta$. The two peaks appearing in the current are due to the two orbitals (with energies ε_1 and ε_2) which are coupled together by V_0. For comparison, the atom's spectral function $A_{d_2}(\omega)$ is shown in a dash-dotted line (in units of the current). Notice how the current resembles the spectral function for smaller values of η. While energy-resolved information can be obtained using derivative spectroscopy with a metal tip,[1,2,6] the SC tip allows one to do so directly from the current. This is due to the energy-filtering arising from the SC tip.

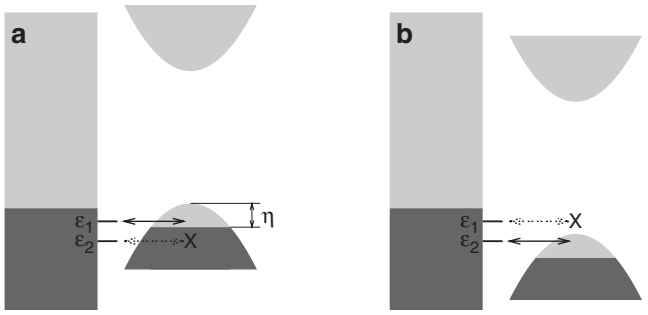

FIG. 3. Schematic illustrating energy-filtered STM. (a) The energy level ε_1 contributes to the current; ε_2 does not. (b) For this bias voltage, ε_2 contributes to the current; ε_1 energy does not, as it lies in the band gap.

The physics behind energy-filtered imaging is shown in Fig. 3. Consider two energy levels ε_1 and ε_2. In Fig. 3(a), ε_1 contributes to the current, while ε_2 does not. By increasing the bias voltage, we obtain the situation shown in Fig. 3(b)—now ε_2 contributes to the current; ε_1 does not, as the bias voltage has raised this energy level into the band gap. However, considering Fig. 2 further, we see that if η becomes too large, the current does not resolve the two peaks in the atom's spectral function. The loss of resolution occurs when the spacing between peaks is approximately equal to η. Hence, a SC STM tip cannot resolve structures in energy that are smaller than η.

For the 3D SC tip, the tunneling current arising for a particular value of η is actually somewhat delicate. As described in the previous paragraph, if η is too large, one loses energy resolution. However, Fig. 2 shows that if η is too small, one loses energy resolution as well. This is because the DOS goes to zero at the top of the valence band in a 3D semiconductor [see Fig. 1(b)]; if η is too small, there are not enough states to produce a current. Hence, for the 3D SC tip, there is a delicate interplay—one needs η large enough to produce a large enough current, but η must also be small enough so that one has an effective energy filter. From Fig. 2, we see that this does not occur with the 1D SC tip; indeed, smaller values of η give better energy resolution. This is due to the singularity in the DOS at the top of the valence band in a 1D semiconductor [see Fig. 1(b)]. The insets of Fig. 2 show the tunneling current for several temperatures. We see that one loses resolution as the temperature is increased. However, the loss of resolution is faster for the 3D SC tip compared to the 1D SC tip.

B. Tunneling current from vibrational modes

Now, we consider the tunneling current arising from the vibrations of an atom attached to a metal surface [Eq. (8)]. In Eqs. (9) and (10), $f=d$; $G_d(\omega)$ is found to be

$$G_d(\omega) = \sum_{n,n'} \sum_{m,m'} f_{n,n'} f^*_{m,m'} G_{nn',m'm}(\omega), \quad (12)$$

with

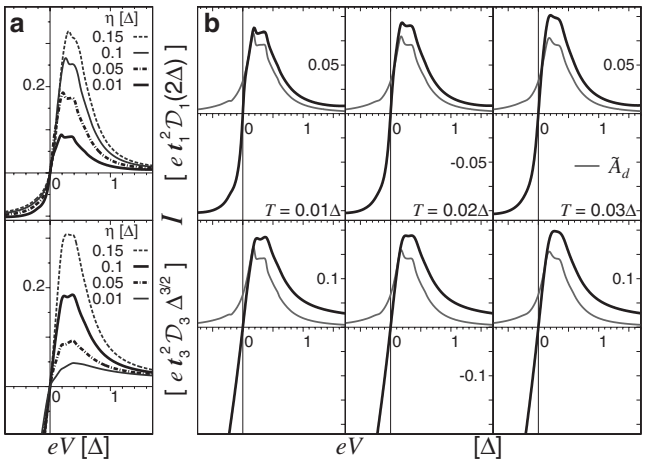

FIG. 4. *I-V* characteristics with a vibrational mode. Parameters: $\tilde{\epsilon}_0=-0.25\Delta$, $\gamma=0.25\Delta$, $\Omega=0.2\Delta$, and $\lambda=0.5$. Top panels: current [in units of $et_1^2\mathcal{D}_1(2\Delta)$] vs bias voltage (in units of Δ) for a 1D SC tip. Bottom panels: current (in units of $et_3^2\mathcal{D}_3\Delta^{3/2}$) vs bias voltage (in units of Δ) for a 3D SC tip. (a) Current for several values of η with $T=0.01\Delta$. (b) Current for several values of T with $\eta=0.01\Delta$ ($\eta=0.1\Delta$) for 1D (3D). $A_d(\omega)$ is shown for comparison in a thin grey line in units of the current and scaled by a factor—$A_d(\omega)$ is in units of $et_1^2\mathcal{D}_1 2\Delta/32\pi$ ($et_3^2\mathcal{D}_3\Delta^{3/2}/16\pi$) for the 1D (3D) SC tip.

$$G_{nn',m'm}(\omega)=\frac{\delta_{m,n}\delta_{m',n'}\{[1-\bar{n}]N_n+\bar{n}N_{n'}\}}{\omega-\epsilon_0+\Omega(n-n')-\Sigma_{n,n'}(\omega)} \tag{13}$$

(see the Appendix for details). Figures 4 and 5 show the tunneling current arising from the vibrations of an atom or molecule. Figure 4 considers the case of strong hybridization between the atom and/or molecule and the surface, and weak coupling to the vibrational mode—the values of the parameters are $\tilde{\epsilon}_0=-0.25\Delta$, $\Omega=0.2\Delta$, $\gamma=0.25\Delta$, and $\lambda=0.5$. Such a value of Ω is relevant to the stretch modes of C_2H_2 (Ref. 10) and CO (Ref. 14) observed by STM via derivative spectroscopy. We see that the current has two peaks—the main peak is due to elastic tunneling and the secondary peak is due to the absorption of a phonon during tunneling. Figure 4(a) shows the current for several values of η. As before, smaller values of η give better energy resolution for the 1D SC tip; the current depends somewhat delicately on η for the 3D SC tip—one loses energy resolution if η is too large or too small. The six panels in Fig. 4(b) show the current for various temperatures. The atom's spectral function $A_d(\omega)$ is shown with a thin gray line for comparison (in units of the current). At the lowest temperature, the current from the 1D SC tip resolves the structure in the atom's spectral function rather accurately for forward bias; it is able to resolve the structure even at higher temperatures. The 3D tip, on the other hand, loses its ability to resolve the structure in the atom's spectral function as the temperature is raised.

Figure 5 shows the tunneling current for the case of weak hybridization between the atom and/or molecule and the surface, and strong coupling to the vibrational mode—the values of the parameters are $\tilde{\epsilon}_0=-0.05\Delta$, $\gamma=0.05\Delta$, $\Omega=0.05\Delta$, and $\lambda=2.0$. Such a value of Ω is relevant to the hindered rotational mode of CO on Cu observed in Ref. 14. Since Ω is small, only small values of η will allow for the structure in the atom's spectral function, which are due to the absorption of phonons during tunneling, to be resolved. The six panels in Fig. 5(b) show the current for various temperatures; as in Fig. 4, the atom's spectral function $A_d(\omega)$ is shown with a thin gray line for comparison. At the lowest temperature, the 1D SC tip resolves most of the structure arising from the phonon mode. Most of the features arising from the vibrational mode are missed with the 3D SC tip. Even at higher temperatures, the current from the 1D SC tip captures the general features of the atom's spectral function.

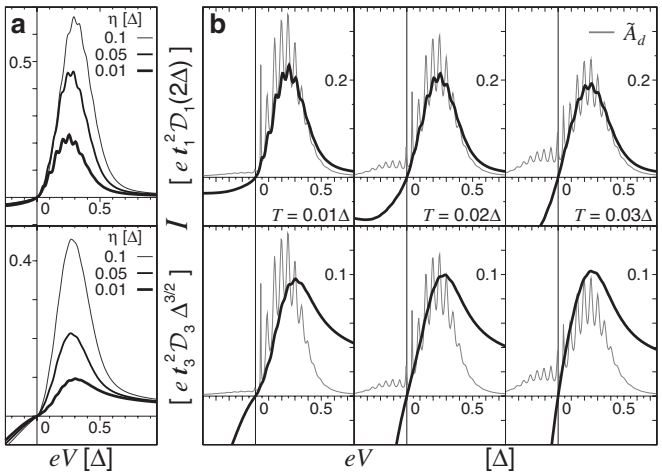

FIG. 5. *I-V* characteristics with a vibrational mode. Parameters: $\tilde{\epsilon}_0=-0.05\Delta$, $\gamma=0.05\Delta$, $\Omega=0.05\Delta$, and $\lambda=2.0$. Top panels: current [in units of $et_1^2\mathcal{D}_1(2\Delta)$] vs voltage (in units of Δ) for a 1D SC tip. Bottom panels: current (in units of $et_3^2\mathcal{D}_3\Delta^{3/2}$) vs voltage (in units of Δ) for a 3D SC tip. (a) Current for several values of η with $T=0.01\Delta$. (b) Current for several values of T with $\eta=0.01\Delta$ ($\eta=0.1\Delta$) for 1D (3D). $A_d(\omega)$ is shown for comparison in a thin gray line in units of the current and scaled by a factor—$A_d(\omega)$ is in units of $et_1^2\mathcal{D}_1 2\Delta/24\pi$ ($et_3^2\mathcal{D}_3\Delta^{3/2}/60\pi$) for the 1D (3D) SC tip.

IV. CONCLUDING REMARKS

In this work, we analyzed models describing an atom or molecule on a metallic surface probed by a SC STM tip; we presented results for the tunneling current from a doped 1D SC STM tip, comparing the results with a doped 3D SC STM tip. A few words are in order about the parameters appearing in our models and calculations. Our models describe the salient features of the systems considered at the energy scales of interest. The parameters in Eqs. (7) (the diatomic molecule) and (8) (the vibrational modes of an atom and/or molecule) were chosen to give realistic and illustrative spectral functions. We were particularly interested in elucidating the factors which influence the achievable energy resolution (see the discussion in Sec. III A). The STM's spectral function, however, deserves further comments. Equation (1) is expected to well describe the DOS of a 1D semiconductor. The STM's spectral function, obtained by convolving Eqs. (1) and (2), captures the salient features where the singularity in the DOS is smoothed by disorder. In our calculations, this smoothing of the singularity was pa-

rameterized by Γ, the (phenomenological) electron scattering rate in Eq. (2). Our models elucidate the behaviors that can arise once Γ is given or, more physically, once the STM's spectral function is specified. *Ab initio* calculations would be desirable to determine the spectral functions for particular materials; such calculations could help determine the materials which would be best suited for use in STM.

To summarize, we considered scanning tunneling microscopy with a doped 1D semiconducting tip. The interplay of band edge physics and the singularity in the density of states allows for energy-filtered STM with high resolution. As mentioned above, while energy-resolved information can be obtained via derivative spectroscopy with a metal STM tip, the 1D semiconducting tip allows one to do so directly from the current. Furthermore, it allows for energy-resolved maps of surface states (with high energy resolution) using only constant-current imaging. A promising place to realize these effects is in doped semiconducting carbon nanotubes.

ACKNOWLEDGMENTS

E.H.K. is grateful to I. R. McNab for bringing Ref. 5 to his attention and for helpful conversations. This work was supported by the NSERC of Canada and a SHARCNET Research Chair.

APPENDIX A: SPECTRAL FUNCTIONS

Here, we outline the calculations for the spectral functions appearing in the expression for the tunneling current [Eq. (9)]—$A_{d_2}(\omega)$ for the diatomic molecule and $A_d(\omega)$ for the vibrational modes of an atom and/or molecule.

1. Diatomic molecule

In Sec. III A, we consider tunneling into atom 2; hence, we need the Green's function [Eq. (10)] with $f=d_2$. A straightforward calculation gives the Fourier transform of Eq. (10) as $[G_{d_2}(\omega)]^{-1}=\omega-\varepsilon_2-\Sigma(\omega)$, where the self-energy is given by

$$\Sigma(\omega)=\Sigma_2(\omega)+\frac{[V_0-\Sigma_{1,2}(\omega)]^2}{\omega-\epsilon_1-\Sigma_1(\omega)}, \tag{A1}$$

with

$$\Sigma_i(\omega)=\sum_{\mathbf{p}}\frac{|V_{\mathbf{p},i}|^2}{\omega-\varepsilon_{\mathbf{p}}+i0^+} \quad (i=1,2),$$

$$\Sigma_{1,2}(\omega)=\sum_{\mathbf{p}}\frac{V_{\mathbf{p},1}V_{\mathbf{p},2}e^{i\mathbf{p}\cdot(\mathbf{r}_1-\mathbf{r}_2)}}{\omega-\varepsilon_{\mathbf{p}}+i0^+}.$$

Using that $V_{\mathbf{p},i}=V_1/\sqrt{\mathrm{Vol}}$ and treating the metal in the wide-band limit, $\Sigma_i(\omega)$ and $\Sigma_{1,2}(\omega)$ are easily computed; we obtain

$$[G_{d_2}(\omega)]^{-1}=\omega-\varepsilon_2+i\gamma-\frac{[V_0-\gamma e^{ik_Fr}/k_Fr]^2}{\omega-\varepsilon_1+i\gamma}, \tag{A2}$$

where k_F is the Fermi wave vector, $r=|\mathbf{r}_2-\mathbf{r}_1|$, and $\gamma=\pi V_1^2\mathcal{D}_0$ ($\mathcal{D}_0$ is the DOS of the metal).

2. Vibrational modes of an atom and/or molecule

As before, we need the Green's function $G_f(\omega)$, where $f=d$. To proceed, we introduce the unitary operator $U=\exp(i\xi pd^\dagger d)$, where $\xi=g/m\Omega^2$. Transforming the Hamiltonian [Eq. (8)], $\tilde{H}=U^\dagger HU$, we obtain

$$\tilde{H}=\sum_{\mathbf{p}}\varepsilon_{\mathbf{p}}c_{\mathbf{p}}^\dagger c_{\mathbf{p}}+\tilde{\epsilon}_0d^\dagger d+\frac{1}{2m}p^2+\frac{m\Omega^2}{2}x^2+\sum_{\mathbf{p}}V_{\mathbf{p}}(e^{i\xi p}c_{\mathbf{p}}^\dagger d+e^{-i\xi p}d^\dagger c_{\mathbf{p}}), \tag{A3}$$

where $\tilde{\epsilon}_0=\varepsilon_0-g^2/2m\Omega^2$. Then, performing the unitary transformation on the Green's function $G_d(\omega)$ [Eq. (10)] and expanding the result in terms of oscillator energy eigenstates,[15] we can write

$$G_d(t)=\sum_{n,n'}\sum_{m,m'}f_{n,n'}f_{m,m'}^*G_{nn',m'm}(t), \tag{A4}$$

where

$$G_{nn',m'm}(t)=-i\Theta(t)\langle\{[d|n\rangle\langle n'|](t),d^\dagger|m'\rangle\langle m'|\}\rangle_{\tilde{H}}, \tag{A5}$$

and $f_{n,n'}=\langle n|e^{i\xi p}|n'\rangle$. ($\langle\ \rangle_{\tilde{H}}$ reminds us that time evolution and matrix elements are computed with respect to $\tilde{H}$.) Explicitly,

$$f_{n,n'}=\sqrt{\frac{\min(n,n')!}{\max(n,n')!}}e^{-\lambda^2/2}(i\lambda)^{|n-n'|}L_{\min(n,n')}^{|n-n'|}(\lambda^2),$$

where $\lambda=g/(\Omega\sqrt{2m\Omega})$ and $L_q^k(z)$ is a Laguerre polynomial.[16] Hence, our problem is to compute the Green's function(s) $G_{nn',m'm}(t)$. To do so, we employ an equations-of-motion approach. Here, we outline the key steps in the calculation; further details can be found in Ref. 15.

Differentiating Eq. (A5) with respect to time, we obtain

$$\begin{aligned}i\partial_tG_{nn',m'm}(t)=&\ \delta(t)[\langle dd^\dagger|n\rangle\langle m|\rangle\delta_{n',m'}+\langle d^\dagger d|m'\rangle\langle n'|\rangle\delta_{n,m}]\\&+[\tilde{\epsilon}_0-\Omega(n-n')]G_{nn',m'm}(t)\\&+\sum_{\mathbf{p},l}V_{\mathbf{p}}[f_{l,n'}^*F_{nl,m'm}^{\mathbf{p}}(t)-f_{n,l}^*A_{ln',m'm}^{\mathbf{p}}(t)\\&+f_{l,n'}^*A_{nl,m'm}^{\mathbf{p}}(t)],\end{aligned} \tag{A6}$$

where $F_{nn',m'm}^{\mathbf{k}}(t)=-i\Theta(t)\langle\{[c_{\mathbf{k}}|n\rangle\langle n'|](t),d^\dagger|m'\rangle\langle m'|\}\rangle_{\tilde{H}}$ and $A_{nn',m'm}^{\mathbf{k}}(t)=-i\Theta(t)\langle\{[d^\dagger c_{\mathbf{k}}d|n\rangle\langle n'|](t),d^\dagger|m'\rangle\langle m'|\}\rangle_{\tilde{H}}$. We then derive the equations of motion for $F_{nn',m'm}^{\mathbf{k}}(t)$ and $A_{nn',m'm}^{\mathbf{k}}(t)$; by ignoring correlations with the metal surface,[15] we obtain a closed set of equations for $G_{nn',m'm}(t)$, $F_{nn',m'm}^{\mathbf{k}}(t)$, and $A_{nn',m'm}^{\mathbf{k}}(t)$. Fourier transforming, one finds $G_{nn',m'm}(\omega)$ and satisfies

$$[\omega - \tilde{\epsilon}_0 + \Omega(n-n')]G_{nn',m'm}(\omega) = \langle dd^\dagger|n\rangle\langle m|\delta_{n',m'} + d^\dagger d|m'\rangle\langle n'|\delta_{m,n}\rangle + \sum_{i,j}[\Lambda^e_{i,n'} f^*_{n,i} f_{j,i} G_{jn',mm'}(\omega) + \Lambda^h_{n,i} f^*_{i,n'} f_{i,j} G_{nj,mm'}(\omega)], \quad \text{(A7)}$$

where

$$\Lambda^e_{nn'}(\omega) = \frac{\gamma}{\pi}\int d\nu \frac{f(\nu)}{\omega - \nu + \Omega(n-n') + i0^+},$$

and $\Lambda^h_{nn'}(\omega) = i\gamma - \Lambda^e_{nn'}(\omega)$, with $\gamma = \pi V_1^2 \mathcal{D}_0$ ($\mathcal{D}_0$ is the DOS of the metal). To make further progress, we approximate Eq. (A7) by setting $j=n$ ($j=n'$) in the first (second) term in the sum. This is justified because the first (second) term in the sum is dominated by $E_{jn'} \simeq E_{nn'}$ ($E_{nj} \simeq E_{nn'}$). Furthermore, we take

$$\langle dd^\dagger|n\rangle\langle m|\delta_{n',m'} + d^\dagger d|m'\rangle\langle n'|\delta_{m,n}\rangle \simeq \delta_{n,m}\delta_{n',m'}\{[1-\bar{n}]N_n + \bar{n}N_{n'}\},$$

where $\bar{n} = \langle d^\dagger d\rangle$ and $N_n = \langle|n\rangle\langle n|\rangle$. These approximations were shown to give very accurate results, compared to the case where the full sum was kept and the expectation values were determined self-consistently.[15] Hence, to good approximation, we obtain

$$G_{nn',m'm}(\omega) = \frac{\delta_{m,n}\delta_{m',n'}\{[1-\bar{n}]N_n + \bar{n}N_{n'}\}}{\omega - \tilde{\epsilon}_0 + \Omega(n-n') - \Sigma_{n,n'}(\omega)}, \quad \text{(A8)}$$

where the self-energy $\Sigma_{n,n'}(\omega)$ is given by

$$\Sigma_{n,n'}(\omega) = -i\gamma - \frac{\gamma}{\pi}\sum_l |f_{n,l}|^2 \psi(z_{l,n'}) - |f_{l,n'}|^2 \psi(z_{n,l}), \quad \text{(A9)}$$

with $\psi(z_{l,l'})$ being the digamma function[16] and

$$z_{l,l'} = \frac{1}{2} - \frac{i}{2\pi T}[\omega + \Omega(l-l')].$$

[1] *Scanning Tunneling Microscopy and Spectroscopy: Theory, Techniques, and Applications*, edited by D. A. Bonnell (Wiley, New York, 2000).

[2] R. Wiesendanger, *Scanning Probe Microscopy and Spectroscopy: Methods and Applications* (Cambridge University Press, Cambridge, 1994).

[3] J. K. Gimzewski and C. Joachim, Science **283**, 1683 (1999).

[4] G. Binnig, H. Rohrer, C. Gerber, and E. Weibel, Appl. Phys. Lett. **40**, 178 (1982); Phys. Rev. Lett. **49**, 57 (1982).

[5] P. Sutter, P. Zahl, E. Sutter, and J. E. Bernard, Phys. Rev. Lett. **90**, 166101 (2003).

[6] G. D. Mahan, *Many Particle Physics* (Plenum, New York, 1990).

[7] J. Gao, Q. Sun, X. C. Xie, and H. Gao, Phys. Rev. B **73**, 235421 (2006).

[8] C. Dekker, Phys. Today **52** (5), 22 (1999); Phys. World **13** (6) (2000); R. Saito, G. Dresselhaus, and M. S. Dresselhaus, *Physical Properties of Carbon Nanotubes* (Imperial College, London, 1998).

[9] T. Shimizu, H. Tokumoto, S. Akita, and Y. Nakayama, Surf. Sci. **486**, L455 (2001).

[10] B. C. Stipe, M. A. Rezaei, and W. Ho, Science **280**, 1732 (1998).

[11] For reviews, see C. Joachim, J. K. Gimzewski, and A. Aviram, Nature (London) **408**, 541 (2000); *Molecular Electronics: Science and Technology*, edited by A. Aviram and M. Ratner (Annals of the New York Academy of Sciences, New York, 1998), Vol. 852.

[12] H. Park, J. Park, A. K. L. Lim, E. H. Anderson, A. P. Alivisatos, and P. L. McEuen, Nature (London) **407**, 57 (2000); N. B. Zhitenev, H. Meng, and Z. Bao, Phys. Rev. Lett. **88**, 226801 (2002).

[13] B. N. J. Persson and A. Baratoff, Phys. Rev. Lett. **59**, 339 (1987).

[14] J. R. Hahn and W. Ho, Phys. Rev. Lett. **87**, 196102 (2001).

[15] K. Flensberg, Phys. Rev. B **68**, 205323 (2003).

[16] I. S. Gradshteyn and I. M. Ryzhik, *Table of Integrals, Series, and Products* (Academic, San Diego, 1994).